Structural and optical studies of ZnS nanocrystal films prepared by sulfosalicylic acid (C$_7$H$_6$O$_6$S)-assisted galvanostatic deposition with subsequent annealing

Xinhua Xu [a,b,c], Feng Wang [a,b,*], Jingjun Liu [a,b], Zhilin Li [a,b], Jing Ji [a,b], Jianfeng Chen [c]

[a] State Key Laboratory of Chemical Resource Engineering, Beijing University of Chemical Technology, Beijing 100029, PR China
[b] College of Materials Science and Engineering, Beijing University of Chemical Technology, Beijing 100029, PR China
[c] State Key Laboratory of Organic–Inorganic Composites, Beijing University of Chemical Technology, Beijing 100029, PR China

ARTICLE INFO

ABSTRACT

Zinc sulfide (ZnS) semiconductor nanocrystal films have been prepared on indium tin oxide coated glass substrates by sulfosalicylic acid (C$_7$H$_6$O$_6$S)-assisted galvanostatic deposition with subsequent annealing. The deposition was performed at 10 mA cm^{-2} in acidic electrolytes containing 15–30 mM Zn(CH$_3$COO)$_2$, 20 mM Na$_2$S$_2$O$_3$, 200 mM LiCl, 0.375 mM Na$_2$SO$_3$, and 0 or 0.2 mM C$_7$H$_6$O$_6$S. Results show that the presence of C$_7$H$_6$O$_6$S can suppress the precipitation of Zn and S impurity phases during the ZnS deposition process. As the [C$_7$H$_6$O$_6$S] = 0.2 mM and [Zn^{2+}] = 20 mM, the deposited ZnS film exhibits only hexagonal structure with an ideal Zn/S atomic ratio of 1.03 and a close-packed granular morphology. But its band gap about 2.86 eV is narrower than the common value of ZnS, probably due to the existence of some spurious acetate species and defect states. By annealing the film at 400 °C for 60 min, its band gap increased up to 3.70 eV, despite that its crystalline phase transformed into cubic structure which usually shows the narrower band gap than hexagonal ZnS. The significant band gap widening could be ascribed to the degradation of spurious acetate species and the reduction of various possible defect states in the annealing process.

© 2012 Elsevier B.V. All rights reserved.

1. Introduction

Zinc sulfide (ZnS) is an important II–VI group semiconductor material occurring in nature as hexagonal wurtzite or cubic sphalerite structure [1]. At room temperature, it has a wide band gap of 3.74–3.91 eV for the hexagonal phase [2,3] and 3.54–3.72 eV for the cubic phase [2–5], corresponding to a band edge of 317–331 nm and 333–350 nm, respectively. Thus no matter what the phase structure is, ZnS would exhibit a considerable adsorption of ultraviolet light at wavelengths lower than the corresponding band edge, while a wide transmittance at the higher wavelengths usually from the near-band-edge ultraviolet region to the deep infrared region [6]. This characteristic of ZnS makes it particularly suitable for the application in thin-film optoelectronic devices, such as solar selective decorative coating [7], phosphors of field emission displays [8], and window layer of solar cells [9] and so on. In addition to the unique optical role, ZnS can prevent these thin-film devices from overheating, thereby ensuring their thermal stabilities in practical applications [10]. In case that the average crystallite size of ZnS film achieves to nanometer range like nanocrystal, the physical properties mentioned above will be profoundly modified [11]. These advantages in combination with its abundant resource and

environmental compatibility make ZnS nanocrystal films attract great attention in both academic and industrial research laboratories.

So far, a variety of techniques such as chemical vapor deposition (CVD) [6,12], chemical bath deposition (CBD) [13,14], spray pyrolysis [15], sputtering [16] and electrodeposition [17,18] have been employed to prepare ZnS nanocrystal films. Among them, CVD and CBD techniques are the most two popular methods due to the possibility of large-area deposition at low cost [6,13]. However, the CVD method usually consists of thermal decomposition of H$_2$S gas and reaction of the S atoms with Zn gas atoms at temperatures above 550 °C [6], which probably have a negative influence on environment. Although the CBD method has no such problem, the resulting films are always poorly crystallized and are not easy in stoichiometry composition [6,13]. Therefore, both of them are not suitable for the large-scale fabrication of high-quality ZnS nanocrystal films and it is necessary to exploit other approaches to fulfill this requirement.

Actually, the electrodeposition is a most promising candidate, which has been used frequently to deposit large area polycrystalline metal chalcogenide thin films such as CdTe [19], SnS [20], CuInSe$_2$ [21], CuInS$_2$ [22], etc. Nevertheless, only several research groups have adopted this technique to prepare ZnS nanocrystal films. For instance, Kassim et al. [17] reported a potentiostatic electrodeposition of cubic ZnS films in an acidic electrolyte containing ZnCl$_2$, Na$_2$S$_2$O$_3$ and triethanolamine, while Murali et al. [18] reported a pulse electrodeposition of hexagonal ZnS films from an acidic electrolyte of ZnSO$_4$ and Na$_2$S$_2$O$_3$. Both of the two reports exposed some problems like the

* Corresponding author at: State Key Laboratory of Chemical Resource Engineering, Beijing University of Chemical Technology, Beijing 100029, PR China. Tel./fax: +86 10 64451996.
E-mail address: wangf@mail.buct.edu.cn (F. Wang).

instability of electrolytes or the nonstoichiometric composition and poor crystallinity of the resulting films. These unfavorable results perhaps can be attributed to the much more positive Nernst potential of sulfur than that of zinc ($E(S_2O_3^{2-}/S) \approx 0.2588$ V, $E(Zn^{2+}/Zn) \approx -1.004$ V, here both the potentials are relative to standard calomel electrode), which could cause the preferential deposition of sulfur and consequently affect the qualities of the obtained ZnS semiconductor films.

Therefore, a great deal of effort is now required to improve the qualities of ZnS nanocrystal films by modifying the electrodeposition technique. Herein, we present a facile approach to prepare ZnS nanocrystal films by galvanostatic deposition from an acidic electrolyte containing $Zn(CH_3COO)_2$, $Na_2S_2O_3$, LiCl, Na_2SO_3 and sulfosalicylic acid ($C_7H_6O_6S$). The $Zn(CH_3COO)_2$, $Na_2S_2O_3$ and LiCl were used as a zinc source, a sulfur source and a supporting electrolyte, respectively. The Na_2SO_3 was used as a stabilizing agent to keep the relative long lifetime of the acidic electrolyte, because it can prevent the formation of sulfur colloids based on the two reactions $S_2O_3^{2-} + 2H^+ \rightarrow S + H_2SO_3$ and $S + SO_3^{2-} \rightarrow S_2O_3^{2-}$ [23]. Characteristically, the $C_7H_6O_6S$ was used as an additive in hopes of narrowing the potential gap of zinc and sulfur. A series of films were deposited with or without the assistance of $C_7H_6O_6S$ additive. The structures, compositions, morphologies and optical properties of these films were characterized and discussed in detail.

2. Experimental details

ZnS nanocrystal films were prepared on indium tin oxide (ITO) coated glass sheets by galvanostatic deposition from acidic electrolytes (pH = 3.5) containing 15–30 mM $Zn(CH_3COO)_2$, 20 mM $Na_2S_2O_3$, 200 mM LiCl, 0.375 mM Na_2SO_3, and 0 or 0.2 mM $C_7H_6O_6S$. Each deposition was performed in a typical two-electrode cell, using the ITO sheet with an exposed area of 3 cm^2 as the working electrode and a Pt sheet with a comparable area as the counter electrode. Prior to the deposition, the two electrodes were ultrasonically cleaned with acetone and distilled water for 30 min in turn. Then the deposition was conducted at a current density of 10 mA cm^{-2} and a temperature of 30 °C for 10 min. In the end, eight films in total were deposited from eight sets of electrolytes with variation of $[Zn^{2+}]$, four ones were obtained without assistance of $C_7H_6O_6S$ and were labeled with (a)–(d), while the other four ones were obtained with the assistance of 0.2 mM $C_7H_6O_6S$ and were marked as (a)′–(d)′.

Crystalline structures of the films were characterized by X-ray diffraction (XRD, Dmax2, Rigaku, Japan) with Cu Kα radiation (λ = 1.54 Å) at 35 kV and 25 mA and a scanning rate of 0.04°/s in the 2 theta range of 10° to 70°. Atomic compositions were investigated by energy dispersive X-ray analysis (EDX, INCA-Penta-FET-X3, Oxford, England) at a SEM operating multiple of 2000. Surface morphologies were observed by scanning electron microscopy (SEM, FE-JSM-6701F, JEOL, Japan) at an operating voltage of 5 kV. Transmittance and reflectance spectra were recorded on a UV–visible–NIR spectrophotometer (UV-3150, Shimadzu, Japan) from 200 to 900 nm. Based on the spectra data, optical band gap E_g of the films were evaluated by the well-known Tauc equation $(\alpha h\nu)^2 = A(h\nu - E_g)$ and the relation $\alpha = (1/d)\ln[(1-R)/T]$ [24,25], where A is a constant, $h\nu$ is photon energy, α is absorption coefficient related to the tested films' transmittance T, reflectance R and thickness d. Infrared spectroscopic studies were conducted on a FT-IR spectrometer (spectrum 100, PerkinElmer, USA).

3. Results and discussion

3.1. Structures and compositions

Fig. 1 shows the XRD patterns of the resulting films. It is observed that all the films deposited at $[C_7H_6O_6S] = 0$ mM and $[Zn^{2+}] = 15$–30 mM (Fig. 1a (a)–(d)) exhibit three obvious diffraction peaks at $2\theta = 26.9°$, 30.2° and 39.8°, corresponding to the (100), (101) and (102) reflections of hexagonal ZnS, respectively (JCPDS Card File, 36–1450). Besides, the

film deposited at $[Zn^{2+}] = 30$ mM exhibits a small cubic ZnS peak at $2\theta = 33.1°$, which is indexed to the (200) reflection of cubic ZnS (JCPDS Card File, 05-0566). Furthermore, it is noticed that all the films present a series of small peaks between 35° and 70°, implying the appearance of Zn (JCPDS Card File, 04-0831) and S (JCPDS Card File, 08-0247) impurity phases.

As 0.2 mM $C_7H_6O_6S$ was added to the initial electrolytes, the peaks of Zn and S disappeared or became lower in the XRD patterns of the deposited films (Fig. 1b (a)′–(d)′), suggesting that the $C_7H_6O_6S$ can inhibit the precipitation of Zn and S impurity phases. In the case of $[Zn^{2+}] = 15$ and 20 mM, the films crystallized with only hexagonal ZnS phase. While, as the $[Zn^{2+}]$ increased to 25 and 30 mM, the films showed a mixture of hexagonal and cubic ZnS as well as trace amounts of Zn and S. The atomic compositions (Zn/S) of the films (a)′–(d)′, estimated by EDX analysis, lie in a range of 0.92–1.20, showing different degrees of deviations from stoichiometry, which is a common phenomenon for semiconductors [26]. By comparison, the film (b)′ with only hexagonal ZnS phase has the relatively ideal atomic ratio (Zn/S) of 1.03. Using Scherrer equation [27], its average crystallite size was estimated to be ca. 45.5 nm based on the FWHM of the most intense XRD diffraction peak (101).

3.2. Surface morphologies

The SEM images, shown in Fig. 2, reveal that all the films (a)′–(d)′ deposited with the assistance of $C_7H_6O_6S$ have a granular morphological feature. Compared with the mixed-phase films (c)′ and (d)′, the hexagonal-phase ZnS films (a)′ and (b)′ especially (b)′ present a relatively close-packed surface. The close-packed surfaces combined with the only hexagonal crystal boundaries would be beneficial for the transport of light-generated carriers [28].
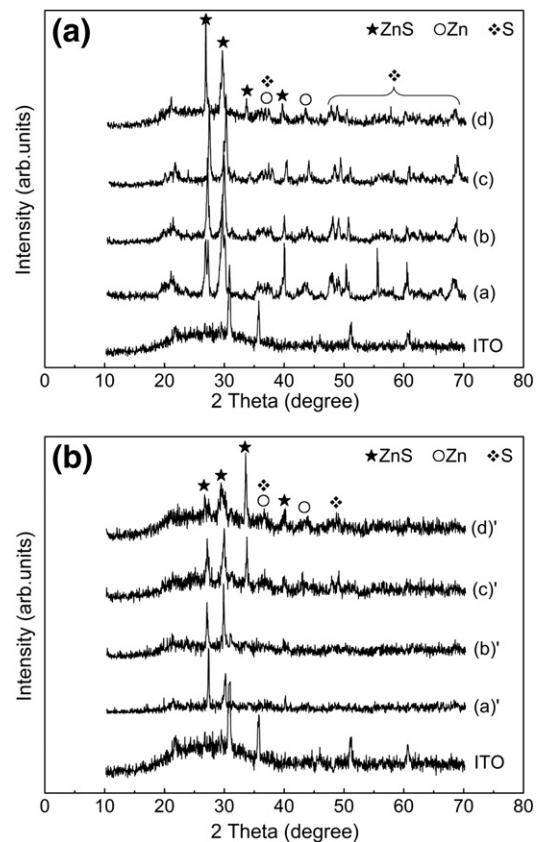

Fig. 1. (a): XRD patterns of the films (a), (b), (c) and (d) deposited from electrolytes with initial $[Zn^{2+}] = 15$, 20, 25 and 30 mM but without $C_7H_6O_6S$, respectively. (b): XRD patterns of the films (a)′, (b)′, (c)′ and (d)′ deposited from the above basic electrolytes with the assistance of 0.2 mM $C_7H_6O_6S$.